THE LASER-INDUCED FORMATION OF PLASMA BUBBLES IN WATER – ELECTROCHEMICAL MEASUREMENTS

HM Hirsimäki School of Chemistry, University of Southampton, Southampton, SO17 1BJ, UK
PR Birkin School of Chemistry, University of Southampton, Southampton, SO17 1BJ, UK
JG Frey School of Chemistry, University of Southampton, Southampton, SO17 1BJ, UK
TG Leighton ISVR, University of Southampton, Southampton, SO17 1BJ, UK

1 INTRODUCTION

The erosion of a surface was a key parameter in the discovery of cavitation around the turn of the 20th century. Since this time, cavitation has been investigated in a multidisciplinary research effort with many exciting and varied applications of this phenomena, ranging from light emission to unusual radical chemistry[1-5]. While there are many benefits of cavitation, it can also be detrimental if produced around sensitive equipment or structures. Indeed erosion of solid surfaces as a result of cavitation action can accelerate the corrosion[6, 7] of that material and ultimately the failure of the structure. Hence it is desirable to study these erosion processes and understand the exact action of cavitation in terms of its erosive potential. Many studies have been performed along these lines. However, there are a variety of ways to generate cavitation, and indeed different types of cavitation that can be created[2]. Hence care must be taken in the interpretation of these different experiments, because the exact erosive mechanism employed in each case may be substantially different. For example the generation of cavitation through acoustic excitation of pre-existing bubble nuclei has been shown to erode surfaces[8-12]. However, in this environment cluster cavitation effects and cloud collapse have been suggested to contribute to the erosive mechanism[13-15]. Alternatively single cavitation events, produced through either laser or spark discharge into a liquid media, are reliant on the effects of a single bubble[13-18] rather than the collective effect that will be generated in a multibubble cloud. While our understanding of the cavitation process has been greatly enhanced by the study of single shot experiments, it must be remembered that, in many ways, the multibubble cloud has more relevance to the industrial scenario where processing of material or the destruction of organics may be desired. Nevertheless the erosion damage from individual cavitation events has been attributed to shock wave and microjet impact on the solid surface in close proximity to the cavitation event. Indeed the exact erosion mechanism has been studied as a function of the dimensionless distance (defined as s/R_{max} where s and R_{max} are the distance between the bubble centre and the solid interface and the maximum bubble radius respectively) between the event and the solid/liquid interface. The resulting erosion damage has in most cases been observed as mass or volume loss with localised *ex-situ* photography of the individual damage associated with jet or shock wave impact[17, 19]. Prolonged exposure of materials, such as various metals, to cavitation has been shown to produce a variety of different forms of material changes. These include sub-surface void formation, grain boundary delineareation, and slip bands[20]. These effects have been compared to shock loading of the material, and have been associated with the bulk properties of the metal including the crystal phase of the material employed[20].

Electrochemical investigation of the effects of cavitation on surfaces has also been performed[8, 9, 21, 22]. The effects of high intensity ultrasound on metal oxide films, glassy carbon, platinum and aluminium and on polymer films deposited on to the surface on electrodes have been studied electrochemically. However, these studies have been partly performed *ex–situ,* with the erosion effects studied after the exposure of the material to cavitation has stopped[17]. Amongst the electrochemical investigations, the work performed by Perusich *et al.* on oxide film erosion is noteworthy[8]. These authors showed an erosion/corrosion effect of ultrasound on an oxide covered electrode, however, they did not investigate the individual effects of single cavitation bubbles. Clearly it would be interesting to observe single surface erosion effects of single cavitation events *in-situ* and with high temporal and spatial resolution[9, 11].

Investigations of the erosion/corrosion of many metals due to multiple bubble events can be found in the literature[20]. Our motivation was to study the effect of individual cavitation bubbles on electrochemical processes. As part of this study, we initially concentrated on mass transfer effects of ultrasound[23]. These studies showed that it was possible to record the individual effects of cavitation events on mass transfer to a solid surface electrochemically. Mass transfer enhancements due to ultrasound can be attributed to a variety of mechanisms produced as a result of the exposure of the liquid to an acoustic field. These include collapse of cavitation bubbles near the solid surface to produce microjets directed at the surface, inertial cavitation of spherical bubbles, the translation or pulsation or shape oscillation of bubbles in the proximity of the electrode, microstreaming and acoustic streaming[24-29]. However, surface effects are only associated with microjet impact and shock wave impact (a direct result of the collapse phase of an inertial (transient) cavitation bubble) onto the solid surface[17]. In order to study these surface erosion effects we have employed a microelectrode in close proximity to an operating ultrasonic cell disrupter[30]. The employment of a 125 or 50 μm diameter electrode(s) is advantageous for the study of mass transfer and surface erosion events produced by individual cavitation bubbles when compared to larger electrodes. The size and electrochemical characteristics of these electrodes facilitates the observation of the effects of individual cavitation events with high spatial and temporal resolution. The results of our preliminary study of laser induced cavitation are now presented.

2 EXPERIMENTAL

Cavitation bubbles were generated by focusing an electro-optically Q-switched Nd:YAG laser (Continuum Surelite NY 61 and Continuum SL II-10, Photonics Solutions PLC) into an electrochemical cell. The laser produced 5 ns pulses at the wavelength of 532 nm and delivered energies up to 260 and 170 mJ per pulse. The beam diameter was 6 mm. The beam was typically first expanded with a concave lens L_3 (Comar optics, f = -40 mm or -25 mm, where f represents the focal length), then collimated with a convex lens L_2 (Comar optics, f = 150 mm) and finally focused with another convex lens L_1 (Mellesgriot, f = 18 mm) that was mounted onto the front window of the electrochemical cell (see figure 1). The electrochemical cell had four windows, access for the working electrodes from the top and separate holders for the reference and counter electrode. The laser power was adjusted by changing the Q-switch delay. A powermeter (Coherent Fieldmaster) was employed to measure the applied power as a function of the Q-switch setting.

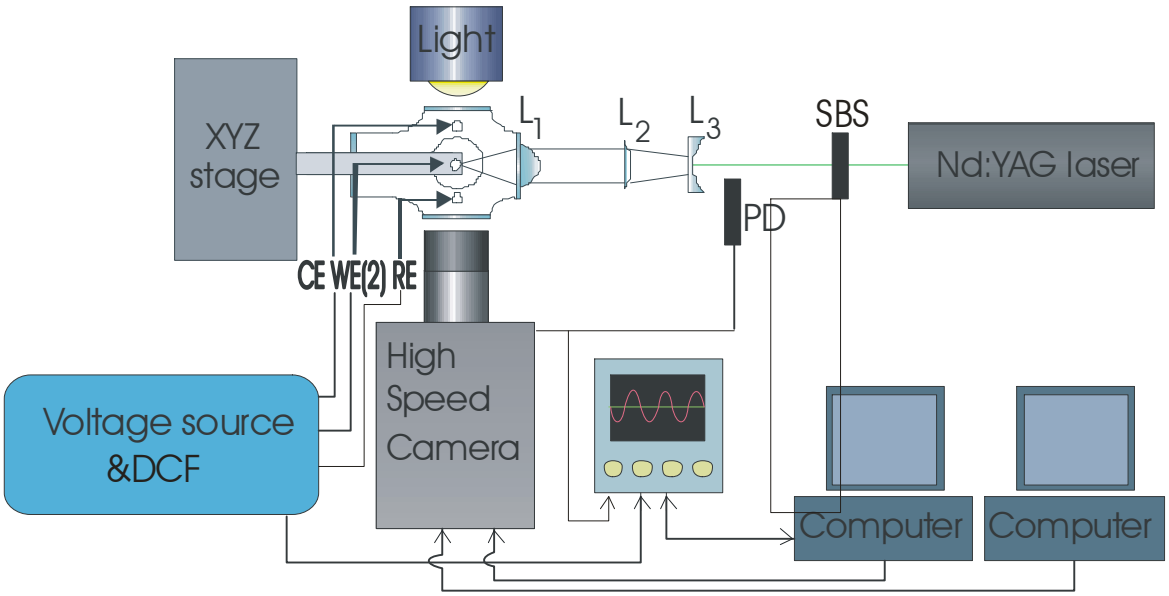

Figure 1. Schematic of the experimental arrangement used for the electrochemical investigation of single laser generated cavitation bubbles. Note DCF represents the dual current follower and SBS a solenoid operated beam stopper.

The electrochemical sensor consists of a so-called 'dual microelectrode'. Such devices, invented at Southampton, consists of two microelectrodes, housed close to each other in a common body of insulator[11, 30]. One electrode senses erosion, and the other simultaneously monitors the mass flux. Clearly since it is the presence of a passive layer which makes an electrode responsive to erosion, the choice of materials for the two electrodes used in this study is important: a 125 μm diameter Pb electrode is used to measure surface erosion, and a 50 μm diameter Pt electrode is employed to measure the mass transfer enhancement, following the generation of a single bubble by a laser. Figure 2 shows a SEM of the two electrodes. The electrodes were sealed together in a single cylinder, having an outer diameter ~2.3 mm. The insulating substrate in this case was Epofix Resin (Struers). Platinum gauze served as the counter electrode and a saturated calomel electrode (SCE) was used as the reference.

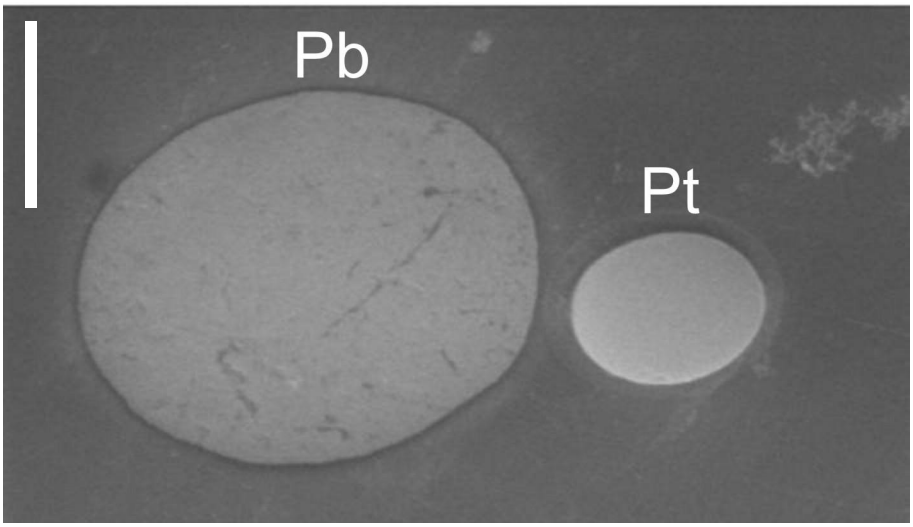

Figure 2. Scanning electron micrograph of a dual microelectrode. The scale bar represents 50 μm.

The electrodes are placed in an electrolyte solution containing a suitable background electrolyte (in this case Na_2SO_4) and a solution soluble redox species (specifically $K_4[Fe(CN)_6]$). In this environment and by electrochemical control of the potential of the electrodes, the surface of the Pb electrode is oxidised to form an insulating passive $PbSO_4$ layer while the Pt electrode continually oxidises the $[Fe(CN)_6]^{4-}$ species at a mass transfer limited rate (here any $[Fe(CN)_6]^{4-}$ that reaches the surface of the Pt electrode is immediately oxidised). Hence the creation of a cavitation bubble close to this electrode will be characterised in two separate ways. First, any erosion of the $PbSO_4$ layer on the surface of the Pb electrode, caused by the cavitation event, will result in an electrochemical signal (an anodic current) corresponding to the reformation of the passive $PbSO_4$ layer[9]. Second, the motion of the liquid around the bubble (either through its creation or subsequent collapse processes) will cause an anodic current enhancement due to the increased rate of mass transfer of material (specifically $[Fe(CN)_6]^{4-}$ ions) to the Pt electrode surface. In this case the observed signal enhancement is caused by forced convection of the liquid. The relaxation of this event will be dominated by the diffusional characteristics of the electrode employed. In turn this is related to the diffusion coefficient of the redox species employed and the electrode size.

The position of the dual working electrode was controlled by a micropositioner (Time and Precision). The micropositioner had manual 25 mm travel X and Y stages and a motorised 50 mm travel Z stage, all the stages had a 10 μm resolution. The stepper motor was controlled by stepper drive (Parker automation) and in-house written software. The micropositioner was placed on a home built stand and a metal holder for the working electrode was designed and attached to the positioner. The current was measured by in-house built potentiostat that was interfaced with a computer through an ADC card (Talisman electronics, PCI-DAS6040) and software written in-house. The current was also recorded by a Tektronix TDS 2014 4-channel 100 MHz oscilloscope that was triggered by a photodiode (Thorlabs) placed close to the beam path.

The solutions were made up using water from an USF Elga Purelab Option E10 water purification system. Water purified in this manner had a conductivity of below 0.06 μS cm^{-1} and a low organic content (TOC < 30 ppb)[1]. Sodium sulphate (BDH, AnalaR), potassium ferrocyanide (Aldrich, 99%) and potassium iodide (Timstar laboratory suppliers) were used as received. The experiments were performed in an environmentally controlled laboratory temperature 20 ^{o}C.

DRS Hadland Imacon 468 high speed camera was borrowed from the EPSRC instrument pool and employed in the combined electrochemistry/laser/imaging experiments. The camera took pictures at the rates from 1000 fps (frames per second) to 100 million fps and captured 8 images at the time. Each picture could be individually set so that the exposure time of each channel and the inter-frame time between each channel were independent of each other. A 55 mm Nikon lens was fitted to the camera together with one 21 mm extension and two 31 mm extensions to enable to focus the camera to the object. An electrode was used as the object to help focusing. A flashlight was mounted on the opposite side of the cell than the camera and was triggered from the camera. A photodiode was used to detect the passing laser pulse and to trigger the camera and flashlight. A 266 MHz computer running Windows 95 controlled the system. The images were analysed using the dedicated DRS Hadland's software and then downloaded in TIFF format to CD via the CD writer fitted to the PC.

3 RESULTS

Figure 3 shows how the mass transfer enhancement due to repetitive bubble formation close to the electrode surface was recorded as a series of anodic current time transients. In this case the repetition rate of the laser was fixed at 5 Hz. Under these conditions the current time transients are of the order of ~1 μA which corresponds to a mass transfer coefficient of 0.05 cm s^{-1}. This is a relatively small mass transfer enhancement compared to cavitation induced by ultrasound[31]. However, the distance between the bubble and the surface will influence the mass transfer

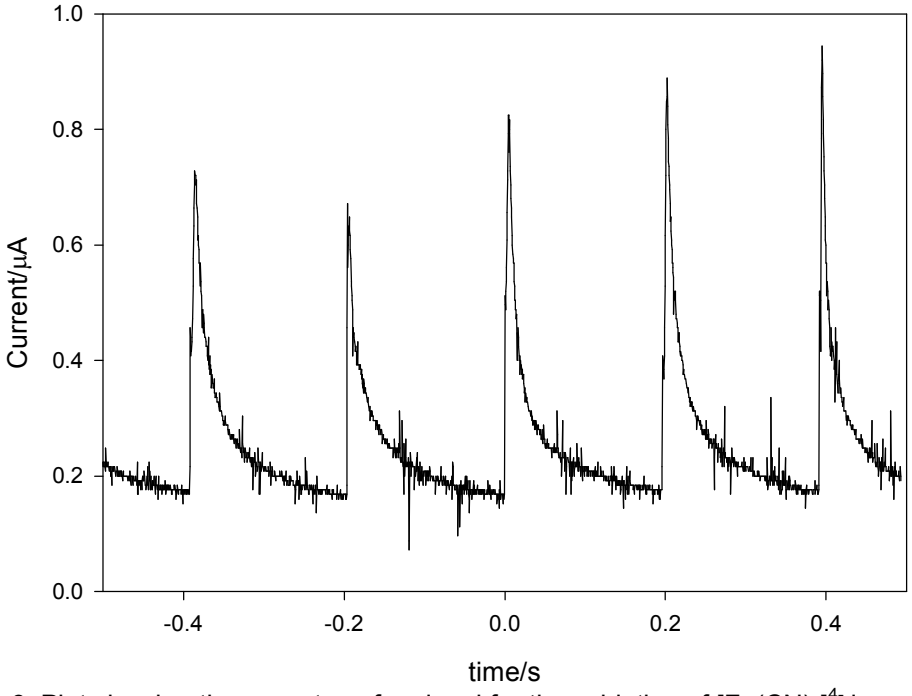

Figure 3. Plot showing the mass transfer signal for the oxidation of $[Fe(CN)_6]^{4-}$ ions at a 50 μm diameter Pt microelectrode in a solution containing 10 mM $K_4Fe(CN)_6$ and 0.75 M Na_2SO_4. The potential of the electrode was held at +0.7 V vs. SCE. The laser repetition rate of the laser was 5 Hz.

[1] manufacturer quoted figure

enhancement recorded at the microelectrode. In order to investigate this effect, a number of experiments were performed using a high–speed camera and the dual microelectrode. Figure 4 shows the images and electrochemical data obtained. Figure 4 (i)-(iv) shows high-speed images of an individual bubble event recorded for 4 separate laser discharges. In each case the distance between the bubble and the electrode was different and is given in the figure legend. Figures 4 (a)-

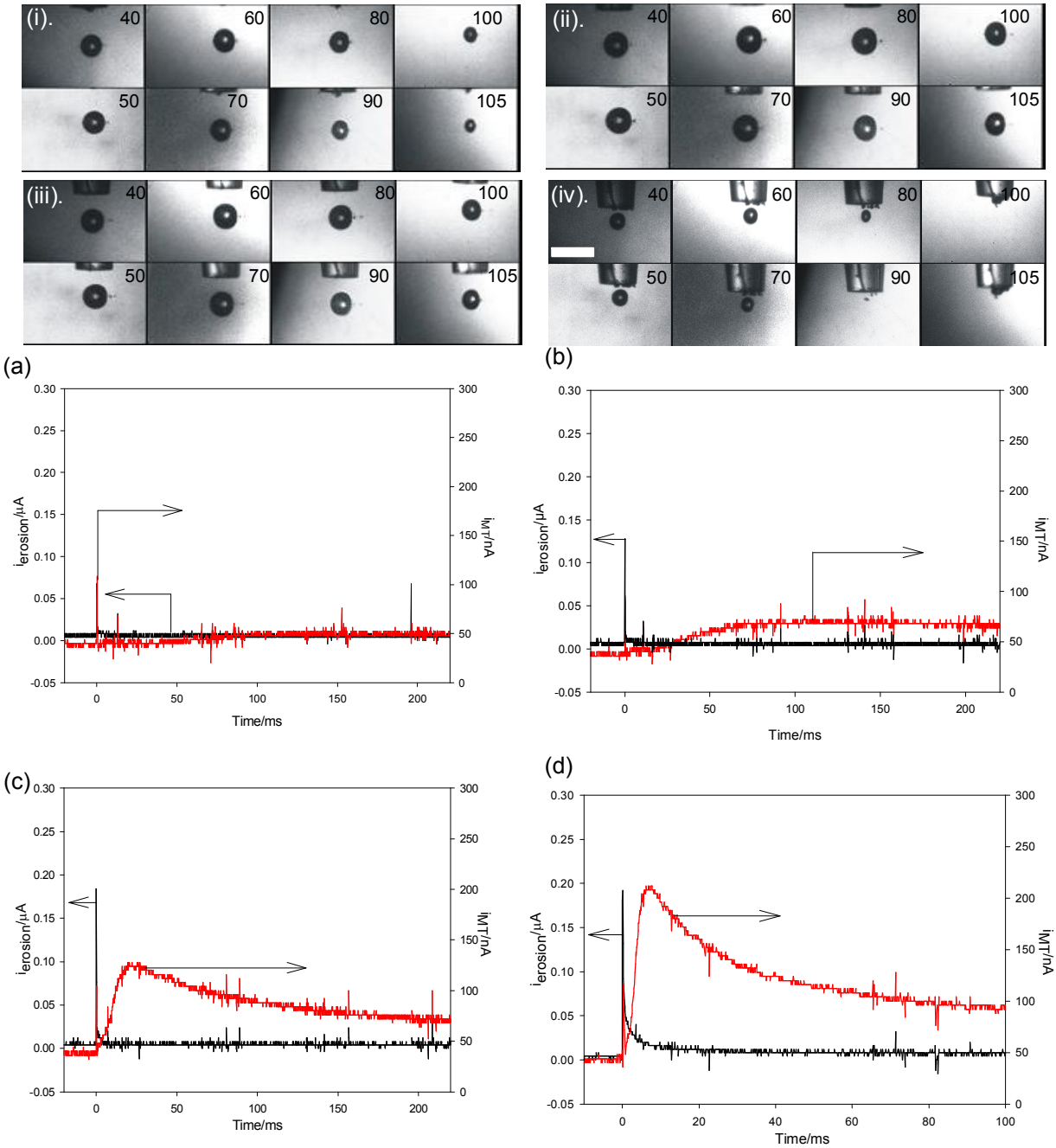

Figure 4. High-speed images and electrochemical signal for mass transfer (▬) and erosion (▬) in a 5 mM $K_4Fe(CN)_6$/0.2 M Na_2SO_4 solution. The potential of the electrodes were held at +0.7 V *vs.* SCE. The distance from the original position (iv) was 1.4 mm, 1.2 mm and 0.8 mm further away from the bubble centre for frames (i), (ii) and (iii) respectively. The time of each image relative to the laser pulse is shown in μs. The scale bar represents 2 mm. The laser energy was approximately 66 mJ/pulse.The electrochemical data shown in (a) – (d) corresponds to images (i) – (iv) respectively.

(d) correspond to the response of the dual electrode to the individual bubble events shown in (i) to (iv) respectively. This experiment clearly demonstrates that the electrochemical signal both from the erosion sensor (the Pb) and the Pt mass transfer sensor are extremely distance dependent as expected. The maximum diameter of the bubbles created in each experiment was ~1 mm although there was some variability in this parameter (see images). As the distance was decreased between the bubble centre and the electrodes, the mass transfer signal and the erosion signal increase markedly with the closet approach (figure 4 (d), (iv)) showing a $\gamma < 2$. Under these circumstances a clear erosion signal is recorded as well as the maximum mass transfer enhancement. However, non-idealities are apparent in these experiments. First, the size of the bubble event was not entirely reproducible (this is also indicated by the varying size of the current time transients shown in figure 3). Second, a number of smaller bubbles could also be generated in addition to the large single event expected. In order to avoid some of these problems degassing and filtering of the liquid was employed.

Figure 5 details the erosion caused by a single cavitation event. It shows the current time trace recorded at a passivated Pb electrode for a single laser pulse. Compared to the data of figure 4, that of figure 5 was taken with increased time resolution and an optimised electrochemical arrangement. A number of transients are apparent. First, at time t = 0 s a large anodic current time transient was observed (labelled L). This occurs at the breakdown of the liquid as the result of laser action. This coincides with the formation of a shock wave as the result of liquid breakdown. In addition two further transients are observed (labelled B_1 and B_2). These are assigned to a bubble collapse process in close proximity to the electrode surface. It is also interesting to note that there are two distinct events shown here. These may be assigned to the erosion of the surface from primary bubble collapse and secondary bubble collapse after rebound. In addition the size of the erosion events indicates that erosion of the surface as a result of liquid breakdown is at least twice as high as the erosion of the surface by bubble action. This poses an interesting question as to the validity of cavitation erosion studies performed through this laser generation method. The electrochemical data presented here suggests that a significant proportion of the damage caused to a solid surface is as the result of liquid breakdown through the action of the laser itself rather than bubble action. This conclusion would not be possible with *ex-situ* investigation of the surface which is commonly employed. However, the electrochemical experiment has the temporal resolution necessary to distinguish between these events and is an *in-situ* technique. Finally the baseline for the electrochemical signal has been shifted away from zero in the time interval between laser shock erosion (L) and the bubble processes (labelled $B_{1,2}$). In this region a small anodic current can be observed (labelled LH). The origin of this event is unclear at this time, but it is possible that heating of the liquid due to the laser pulse could be responsible. It must be remembered that the ~15 mJ pulse of laser energy is focussed to < 1 mm from the surface of the salt passivated Pb solid/liquid interface. Clearly some of this energy results in solution heating. The passivation of the Pb surface relies on the insolubility of the $PbSO_4$ layer. The solubility product, K_{sp}, of $PbSO_4$ is 1.82×10^{-8} at 25 ^{o}C[32]. Hence it is possible to calculate the solubility product as a function of temperature (and hence the concentration of Pb^{2+} at the solid liquid interface) using equation (1)

$$\ln K_{sp} = -\frac{\Delta G^{o}}{RT} \qquad (1)$$

here ΔG^{0} is the Gibbs free energy associated with the process, T the temperature and R the gas constant[32]. This calculation suggests that the solubility of the $PbSO_4$ increases with temperature. However, equating this to the actual local temperature is a non-trivial matter as a number of temperature dependent parameters (e.g. the mass transfer coefficient of the Pb^{2+} ion as a function of temperature and solution flow) as well as the contribution of direct laser heating of the surface need to be known directly. Clearly without supporting experimental evidence a local temperature prediction is difficult to achieve from the data. Nevertheless the presence of the transient labelled 'LH' in figure 5 does suggest that local temperature may be important. Indeed electrochemical experiments using direct focussing of laser energy onto electrode surface to induce rapid temperature changes (but with lower intensities) have been reported in the literature[33-35]. These

provide supporting evidence for the consideration of thermal effects within the experimental environment employed here.

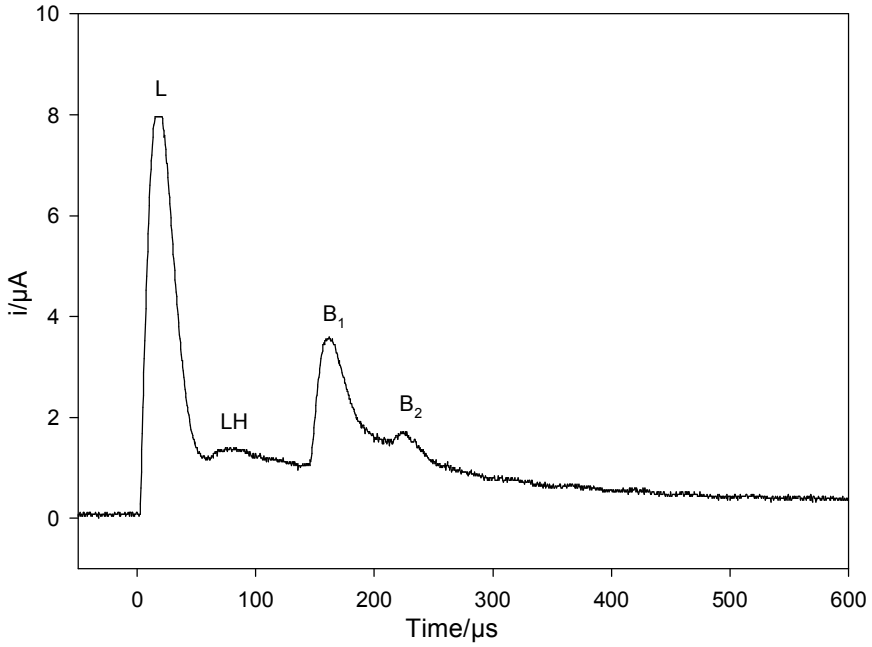

Figure 5. Plot showing the erosion signal recorded for 125 μm diameter Pb electrode exposed to a single laser generated bubble event. The laser was fired at t = 0 s. The solution contained 1 mM KI and 0.2 M Na_2SO_4. The potential of the electrode was held at +0.6 V vs. SCE.

4 CONCLUSIONS

A dual microelectrode has been successfully deployed to study the mass transfer characteristics and the erosion processes that are generated by single large cavitation events. The mass transfer signal suggests that solution motion as a result of bubble generation is produced as expected. High-speed imaging and electrochemical data indicate that the effects on a solid surface are dependent on the bubble to electrode distance as expected. In addition single events are difficult to achieve using a repetitive laser discharge. Other investigations (not shown[36]) have demonstrated that this problem can be circumvented through the use of single shot experiments and the careful preparation of the solutions employed. Preliminary high-time resolution erosion experiments employing a passivated Pb solid/liquid interface have suggested that the erosion of the surface occurs due to laser shock wave generation and bubble collapse. In addition the erosion transient appears complicated by a non-zero baseline which could possibly be due to local heating effects.

5 ACKNOWLEDGEMENTS

We thank the EPSRC and AWE (JGS) for funding for HMH (GR/S01764/01), the Engineering Loan pool for the use of the high-speed camera used in this work and Dr Graham Ball for useful discussions.

6 REFERENCES

1. D. F. Gaitan, L. A. Crum, C. C. Church and R. A. Roy, 'Sonoluminescence and bubble dynamics for a single, stable, cavitation bubble', J. Acoust. Soc. Am., 91, 3166. (1992).
2. T. G. Leighton. The Acoustic Bubble, Academic Press, (1994).
3. A. Henglein, 'Chemical Effects of Continuous and pulsed ultrasound in aqueous solutions.' Ultrasonics Sonochemistry, 2, s115-s121. (1995).
4. A. Henglein, D. Herburger and M. Gutierrez, 'Sonochemistry: some factors that determine the ability of a liquid to cavitate in a ultrasonic field', Journal of Physical Chemistry, 96, 1126. (1992).
5. A. Weissler, 'Formation of hydrogen peroxide by ultrasonic waves: free radicals', Journal of the American Chemical Society, 81, 1077. (1959).
6. G. O. H. Whillock and B. F. Harvey, 'Ultrasonically enhanced Corrosion of 304L Stainless Steel II: The effect of frequency, acoustic power and horn to specimen distance.' Ultrasonics Sonochemistry, 4, 33-38. (1997).
7. G. O. H. Whillock and B. F. Harvey, 'Ultrasonically enhanced corrosion of 304L stainless steel I: The effect of temperature and hydrostatic pressure.' Ultrasonics Sonochemistry, 4, 23-31. (1997).
8. S. A. Perusich and R. C. Alkire, 'Ultrasonically induced cavitation studies of electrochemical passivity and transport mechanisms,
part I', Journal of the Electrochemical Society, 138, 700. (1991).
9. P. R. Birkin, R. O'Connor, C. Rapple and S. Silva-Martinez, 'Electrochemical measurement of erosion from individual cavitation generated from continuous ultrasound', Journal of the Chemical Society Faraday Transactions, 94, 3365-3371. (1998).
10. P. R. Birkin, D. G. Offin, P. F. Joseph and T. G. Leighton, 'Cavitation, shock waves and the invasive nature of sonoelectrochemistry', Journal Of Physical Chemistry B, 109, 16997-17005. (2005).
11. P. R. Birkin, D. G. Offin and T. G. Leighton, 'A novel dual microelectrode for investigating mass transfer and surface erosion caused by cavitation', Electrochemistry Communications, 6, 1174-1179. (2004).
12. P. R. Birkin, D. G. Offin and T. G. Leighton, 'The study of surface processes under electrochemical control in the presence of inertial cavitation', Wear, 258, 623-628. (2005).
13. I. Hansson, V. Kedrinskii and K. A. Morch, 'On the dynamics of cavity clusters', Journal of Physics D: Applied Physics, 15, 1725-1734. (1982).
14. I. Hansson and K. A. Morch, 'The dynamics of cavity clusters in ultrasonic (vibratory) cavitation erosion', Journal of Applied Physics, 51, 4651-4658. (1980).
15. B. Vyas and C. M. Preece, 'Stress produced in a solid by cavitation', Journal of Applied Physics, 47, 5133-5138. (1976).
16. W. Lauternborn and H. Bolle, 'Experimental investigations of cavitation-bubble collapse in the neighbourhood of a solid boundary', J. Fluid Mech., 72, 391. (1975).
17. A. Philip and W. Lauterborn, 'Cavitation erosion by single laser-produced bubbles.' Journal of Fluid Mechanics, 361, 75-116. (1998).
18. Y. Tomita and A. Shima, 'High speed photographic observations of laser induced cavitation bubbles', Acustica, 71, 161-171. (1990).
19. R. P. Tong, W. P. Schiffers, S. J. Shaw, J. R. Blake and D. C. Emmony, 'The role of 'splashing' in the collapse of a laser-generated cavity near a rigid boundary', Journal Of Fluid Mechanics, 380, 339-361. (1999).
20. C. M. Preece and I. L. H. Hansson, Adv. Mech. Phys. Surf., 1, 199-254. (1981).
21. P. R. Birkin, D. G. Offin and T. G. Leighton, 'Experimental and theoretical characterisation of sonochemical cells - Part 2 Cell disruptors (Ultrasonic horns) and cavity cluster collapse', PCCP, 7, 530 - 537. (2005).
22. H. H. Zhang and L. A. Coury, 'Effects of High-Intensity Ultrasound on Glassy-Carbon Electrodes', Analytical Chemistry, 65, 1552-1558. (1993).
23. P. R. Birkin and S. Silva-Martinez, 'The Effect of Ultrasound on Mass Transfer to a Microelectrode.' Journal of the Chemical Society Chemical Communications, 1807 - 1808. (1995).
24. W. E. Rowe and W.L.Nyborg, 'Changes in the Electrode process brought about by small scale acoustic streaming', Journal of the Acoustics Society of America, 39, 965-971. (1966).

25. J. Kolb and W. Nyborg, 'Small-scale acoustic streaming in liquids', J. Acoust. Soc. Am., 28, 1237. (1956).
26. W. L. Nyborg and M.I.L.Seegall, Effects of acoustic microstreaming at electrodes, Proceedings of the 3rd International Congress on Acoustics, Conference, 346-348. (1960).
27. P. R. Birkin, T. G. Leighton, Y. E. Watson and J. F. Power, 'Acoustoelectrochemistry', Acoustics Bulletin, Sept/Oct, 24-37. (2001).
28. P. R. Birkin, Y. E. Watson and T. G. Leighton, 'Efficient mass transfer from an acoustically oscillated gas bubble', Journal of the Chemical Society Chemical Communications, 2650-2651. (2001).
29. P. R. Birkin, Y. E. Watson, T. G. Leighton and K. L. Smith, 'Electrochemical Detection of Faraday Waves on the Surface of a Gas Bubble.' Langmuir, 18, 2135-2140. (2002).
30. D. G. Offin, PhD, An investigation of fast surface re-formation in the presence of inertial (transient) cavitation, University of Southampton, (2006).
31. P. R. Birkin and S. Silva-Martinez, 'A Study of the effect of ultrasound on mass transfer to a microelectrode.' Journal of Electroanalytical Chemistry, 416, 127-138. (1996).
32. CRC. Handbook of Chemistry and Physics 1913-1995, 75th CRC Press, (1995).
33. V. Climent, B. A. Coles, R. G. Compton and J. M. Feliu, 'Coulostatic potential transients induced by laser heating of platinum stepped electrodes: influence of steps on the entropy of double layer formation', Journal of Electroanalytical Chemistry, 561, 157-165. (2004).
34. J. L. Brennan and R. J. Forster, 'Laser light and electrodes: Interaction mechanisms and electroanalytical applications', Journal of Physical Chemistry B, 107, 9344-9350. (2003).
35. J. F. Smalley, M. D. Newton and S. W. Feldberg, 'An informative subtlety of itemperature-jump or coulostatic responses for surface-attached species', Electrochemistry Communications, 2, 832-838. (2000).
36. H. Hirsimäki, PhD, An Electrochemical Investigation of Laser Cavitation, University of Southampton, (2006).